Genome-wide analysis of histone H3.1 and H3.3 variants in *Arabidopsis thaliana*

Hume Stroud[a,1], Sofía Otero[b,1], Bénédicte Desvoyes[b], Elena Ramírez-Parra[b,2], Steven E. Jacobsen[a,c,d,3], and Crisanto Gutierrez[b,3]

[a]Department of Molecular, Cell, and Developmental Biology, University of California, Los Angeles, CA 90095; [b]Centro de Biologia Molecular Severo Ochoa, Consejo Superior de Investigaciones Cientificas, Universidad Autónoma de Madrid, Nicolas Cabrera 1, 28049 Madrid, Spain; [c]Howard Hughes Medical Institute, University of California, Los Angeles, CA 90095; and [d]Eli & Edythe Broad Center of Regenerative Medicine & Stem Cell Research, University of California, Los Angeles, CA 90095

Contributed by Steven E. Jacobsen, February 22, 2012 (sent for review December 12, 2011)

Nucleosomes package eukaryotic DNA and are composed of four different histone proteins, designated H3, H4, H2A, and H2B. Histone H3 has two main variants, H3.1 and H3.3, which show different genomic localization patterns in animals. We profiled H3.1 and H3.3 variants in the genome of the plant *Arabidopsis thaliana* and found that the localization of these variants shows broad similarity in plants and animals, along with some unique features. H3.1 was enriched in silent areas of the genome, including regions containing the repressive chromatin modifications H3 lysine 27 methylation, H3 lysine 9 methylation, and DNA methylation. In contrast, H3.3 was enriched in actively transcribed genes, especially peaking at the 3′ end of genes, and correlated with histone modifications associated with gene activation, such as histone H3 lysine 4 methylation and H2B ubiquitylation, as well as RNA Pol II occupancy. Surprisingly, both H3.1 and H3.3 were enriched on defined origins of replication, as was overall nucleosome density, suggesting a novel characteristic of plant origins. Our results are broadly consistent with the hypothesis that H3.1 acts as the canonical histone that is incorporated during DNA replication, whereas H3.3 acts as the replacement histone that can be incorporated outside of S-phase during chromatin-disrupting processes like transcription.

Nucleosomes, the basic units of chromatin, consist of DNA wrapped around a core of eight histone proteins composed of two dimers of histones H2A and H2B and a tetramer of histones H3 and H4. In multicellular organisms, multiple variants of each histone protein coexist in the same nucleus. In the case of histone H3, three variants are found in both plants and animals: the canonical H3.1, the variant H3.3, and the centromere-specific CENP-A (CENH3) (1, 2). In animals, deposition of the canonical H3.1 into chromatin is generally DNA replication-dependent and occurs in a process mediated by the CAF-1 chaperone, whereas the H3.3 variant is deposited mainly by the HIRA chaperone in a DNA replication-independent manner (3–6).

Plants and animals share the components involved in H3 dynamics, including canonical and variant H3 proteins, gene structures, and the chaperones responsible for their deposition (2, 7). In addition, extensive conservation in the amino acid sequences and expression patterns of histones H3.1 and H3.3 is seen in animals and plants, despite evidence that H3.1 and H3.3 evolved independently in the two kingdoms based on analyses of amino acid sequences (1, 2, 7, 8); for instance, in both plants and animals, H3.3 differs from H3.1 at only three or four amino acid positions (2, 9). Histone H3 variants have been profiled at a genome-wide level in *Drosophila* and mammalian cells (5, 10, 11). Consistent with its DNA replication-independent deposition, H3.3 is enriched in actively transcribed genes. In addition, mass spectrometry studies of posttranslational modifications of human H3.1 showed H3.1 enrichment in the silencing-related H3K9 dimethylation mark (12, 13). A mass spectrometry study of the posttranslational modifications of *Arabidopsis* histone H3.1 and H3.3 revealed H3.1 enrichment in the silencing-related H3K27 methylation marks (H3K27me1, H3K27me2, and H3K27me3) and H3.3 enrichment in the H3K36 methylation marks (H3K36me1, H3K36me2, and H3K36me3) found in the transcribed regions of active genes (14). These results suggest that the H3.1 and H3.3 proteins may demonstrate a similar relationship with transcription as is seen in animals. In this paper, we describe the genome-wide profiling of H3.1 and H3.3 variants in the plant kingdom and show that the patterns are broadly conserved with those in animals with H3.1 enrichment in heterochromatin and H3.3 enrichment in transcriptionally active regions. Our results also reveal the surprising finding that both H3 variants are highly enriched at DNA replication origins.

Results and Discussion

To study the function of canonical and variant H3 proteins, we generated genome-wide maps for H3.1 and H3.3 by chromatin immunoprecipitation followed by massively parallel sequencing (ChIP-seq). For this study, we selected HTR13 as the representative of the cell cycle-regulated canonical H3.1 proteins and HTR5 for the constitutively expressed H3.3 variants, both of which have been described previously (15, 16). We generated Myc-tagged versions of each gene, driven by their respective endogenous promoters, and found that both were well expressed (Fig. S1). We generated high-coverage maps with 75–90 million reads that uniquely mapped to the *Arabidopsis* genome. We examined the distributions of H3.1 and H3.3 across the five *Arabidopsis* chromosomes and found that H3.1 was enriched in pericentromeric heterochromatin (areas of silent chromatin near the centromeres), whereas H3.3 was depleted in these regions (Fig. 1*A*), consistent with published immunofluorescence data (9). Closer examination of the data revealed that certain genes and elements tend to be enriched for either H3.1 or H3.3 (Fig. 1*B*). We describe these patterns in detail below.

Distribution of H3.1. We first sought to examine the relationship between H3.1 and gene expression levels. To determine expression levels of genes from the same tissue that was used for histone variant profiling, we performed RNA sequencing (RNA-seq) from 10-d-old seedlings. The distribution of H3.1 reads over genes with different expression levels revealed an anticorrelation between H3.1 and

Author contributions: H.S., S.O., B.D., E.R.-P., S.E.J., and C.G. designed research; H.S., S.O., and B.D. performed research; H.S., S.O., S.E.J., and C.G. analyzed data; and H.S., S.E.J., and C.G. wrote the paper.

The authors declare no conflict of interest.

Database deposition: The sequences reported in this paper have been deposited in the Gene Expression Omnibus (GEO) database, www.ncbi.nlm.nih.gov/geo (accession no. GSE34840).

[1]H.S. and S.O. contributed equally to this work.

[2]Present address: Centro de Biotecnologia y Genomica de Plantas, Campus de Montegancedo, 28223 Madrid, Spain.

[3]To whom correspondence may be addressed. E-mail: jacobsen@ucla.edu or cgutierrez@cbm.uam.es.

This article contains supporting information online at www.pnas.org/lookup/suppl/doi:10.1073/pnas.1203145109/-/DCSupplemental.

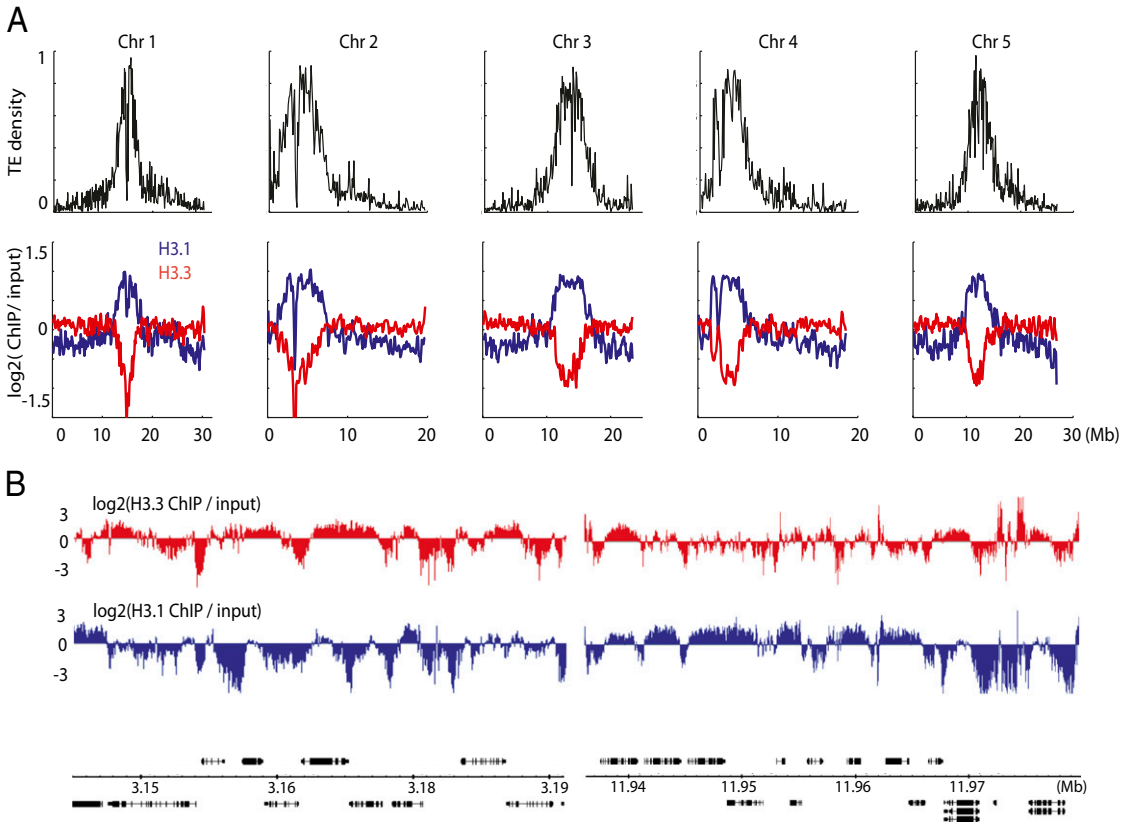

Fig. 1. Genome-wide map of H3.1 and H3.3. (*A*) Chromosomal distributions of H3.1 and H3.3 ChIP-seq reads relative to input genomic DNA. Reads per million mapping reads were calculated in 100-kb bins. Transposable element density was also plotted to indicate locations of pericentromeric heterochromatin. Spikes near the centromeres correspond to regions of low mappability of unique reads. (*B*) Representative genome-browser views of H3.1 and H3.3 in regions of chromosome 1. Genes (black) are also shown.

expression levels, suggesting that H3.1 is associated with silencing (Fig. 2*A*). In addition, H3.1 was enriched over transposable elements, consistent with an association with heterochromatin (Fig. 2*B*).

We also tested whether H3.1 was associated with DNA methylation. We identified a total of 20,097 regions that were significantly enriched with H3.1 (*Materials and Methods*) and examined the DNA methylation levels over these sites using whole genome bisulfite sequencing (BS-seq) data (17). DNA methylation in all sequence contexts (CG, CHG, and CHH, where H = A, T or C) were relatively enriched over H3.1 sites (Fig. 2*C*), indicating a correlation between H3.1 and DNA-methylated sites.

Although most of the heterochromatin in *Arabidopsis* exists near the centromeres, (pericentromeric heterochromatin), small patches of heterochromatin are also seen in the otherwise euchromatic arms of chromosomes. Histone H3 lysine 9 dimethylation (H3K9me2) is a hallmark of heterochromatin and is associated with heterochromatin in both pericentromeric regions and the patches of heterochromatin in the arms (18). To test whether H3.1 is enriched in both of these regions (Fig. 1*A*), we plotted H3.1 enrichment over defined H3K9me2-enriched sites in the arms (19). We found that H3.1 was highly enriched over these sites, suggesting that H3.1 is globally associated with heterochromatin (Fig. 2*D*). Genome browser views of individual locations of small heterochromatin patches also support the association of H3.1 with H3K9me2 (Fig. 2*E*). We noted similar trends between H3.1 and H3K27me1, a chromatin modification generally associated with H3K9me2 (19) (Fig. S2).

H3K27me3, another histone modification associated with gene silencing, is controlled by the polycomb system in plants and animals (20). H3K27me3 is enriched on ~17% of protein-coding genes. These genes are enriched in developmentally important transcription factors (TFs) and generally do not overlap with H3K9me2 and DNA methylation (21, 22). Notably, examination of the distribution of H3.1 over defined H3K27me3 sites showed that H3.1 was highly enriched in H3K27me3 regions (Fig. 2*F*). Genome browser views of individual genomic locations also suggest a strong association of H3.1 with H3K27me3 (Fig. 2*G*). These results support the view that H3.1 is enriched in areas of the genome that are transcriptionally silent and are marked by either DNA methylation or H3K27me3.

Previous studies have shown that pericentromeric heterochromatin in *Arabidopsis* is enriched in overall nucleosome content as evaluated by micrococcal nuclease mapping of nucleosomes (Nuc-seq) and by measuring the total histone H3 content using an antibody against the unmodified C terminus of H3 (H3 ChIP-seq) (23). Given the close association between H3.1 and repressive histone modifications, we asked whether H3K9me2 and H3K27me3 sites are generally enriched in nucleosomes, using genome-wide H3 ChIP-seq, Nuc-seq, and a theoretical nucleosome prediction algorithm (24). We found that both H3K9me2 and H3K27me3 sites are enriched with nucleosomes (Fig. 2 *H* and *I*), which is consistent with our finding that these regions were highly enriched in H3.1.

Taken together, our results show that H3.1 is associated with transcriptionally silent regions in the genome, which tend to be densely packed with nucleosomes.

Distribution of H3.3. Unlike H3.1, H3.3 was not associated with silencing marks, such as H3K9me2 and H3K27me3 (Fig. 2 *D*–*G*). We examined the distribution of H3.3 over genes with different

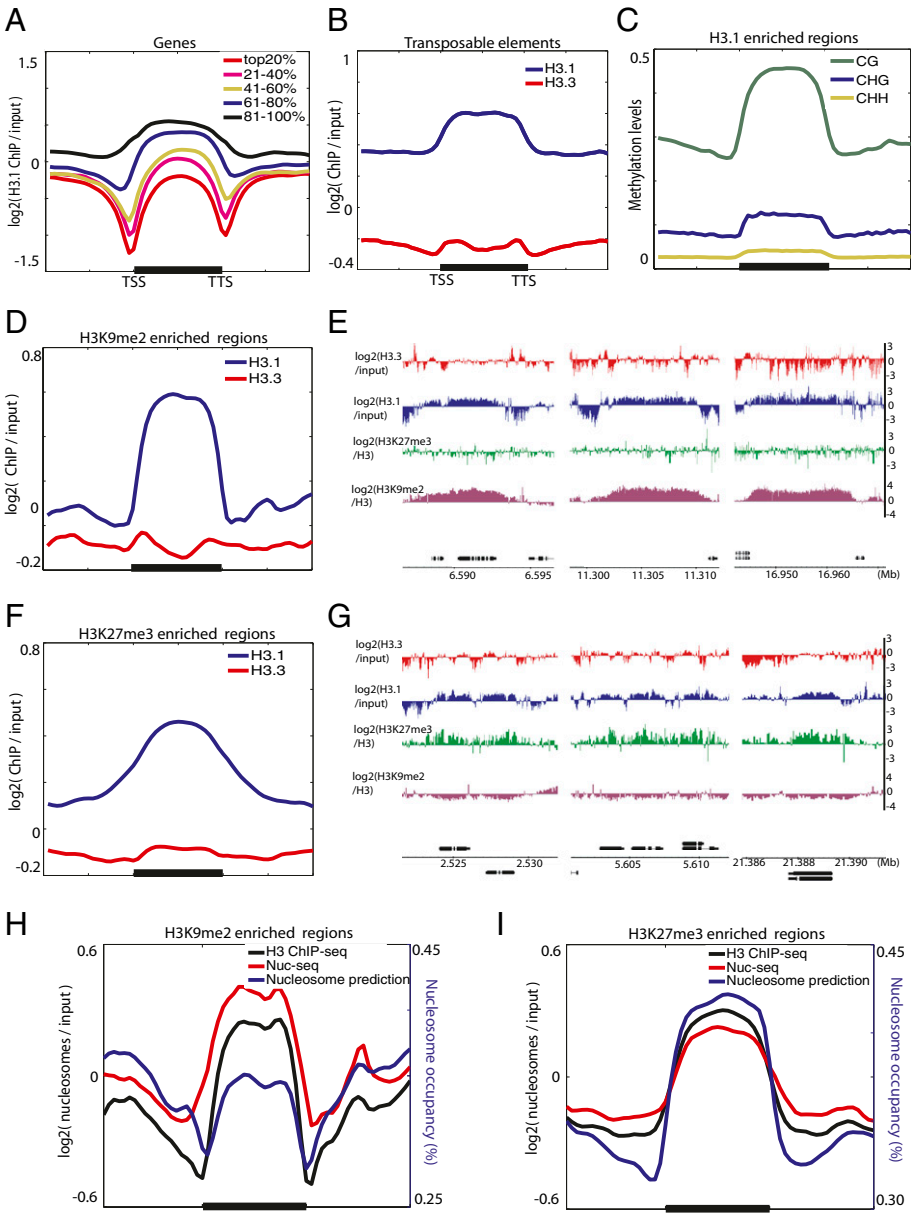

Fig. 2. Genome-wide distribution of H3.1. (*A*) Anticorrelation of H3.1 and gene expression levels. Flanking regions are the same length as the gene body (middle region). (*B*) Transposable elements (TE). Flanking regions are the same length as the TE (middle region). (*C*) Pattern of DNA methylation over H3.1-enriched regions. Flanking regions are the same length as the H3.1 region (middle region). (*D*) Distribution of H3.1 and H3.3 over defined H3K9me2 sites in the arms of chromosomes. Flanking regions are the same length as the H3K9me2 region (middle region). (*E*) Genome browser views of H3.1 and H3K9me2 in regions of chromosome 1. Annotated genes are shown as well. (*F*) Distribution of H3.1 and H3.3 over defined H3K27me3 sites. Flanking regions are the same length as the H3K27me3 region (middle region). (*G*) Genome-browser views of H3.1 and H3K27me3 in regions of chromosome 1. (*H* and *I*) Distribution of H3 ChIP-seq, Nuc-seq and predicted nucleosomes occupancies over H3K9me2 (*H*) and H3K27me3 (*I*) regions. Flanking regions are the same length as the H3K9me2 region (middle region).

expression levels and found that H3.3 is positively correlated with gene expression (Fig. 3*A*), demonstrating that H3.3 is associated with active genes. Notably, H3.3 was most highly enriched in the 3′ end of the transcribed region of the genes, similar to what has been reported for H3.3 distribution in *Caenorhabditis elegans* genes (25). This trend was even clearer when we grouped genes of similar sizes and examined the distribution of H3.3 (Fig. 3*B*).

Many *Arabidopsis* genes contain DNA methylation (specifically in CG contexts) within their transcribed regions (i.e., gene body methylation) (26–29). Gene body methylation is widely conserved in eukaryotic organisms (30, 31), although its function remains unknown. Given that gene body methylation tends to be skewed toward the 3′ end of gene bodies, we tested the correlation between H3.3 and DNA methylation. We identified a total of 19,983 regions significantly enriched in H3.3 (*Materials and Methods*). We examined the distribution of DNA methylation over these H3.3-enriched regions and found that H3.3 is preferentially associated with CG methylation, but not with CHG and CHH methylation (Fig. 3*C*).

To further investigate the association of H3.3 with gene body methylation, we examined the distribution of H3.3 over three previously defined classes of genes: body-methylated genes, unmethylated genes, and promoter-methylated genes (27). We found that H3.3 was preferentially enriched within body-methylated genes (Fig. 3*D*), which likely explains the correlation between H3.3 and CG methylation. In contrast, H3.1 was enriched over promoter-

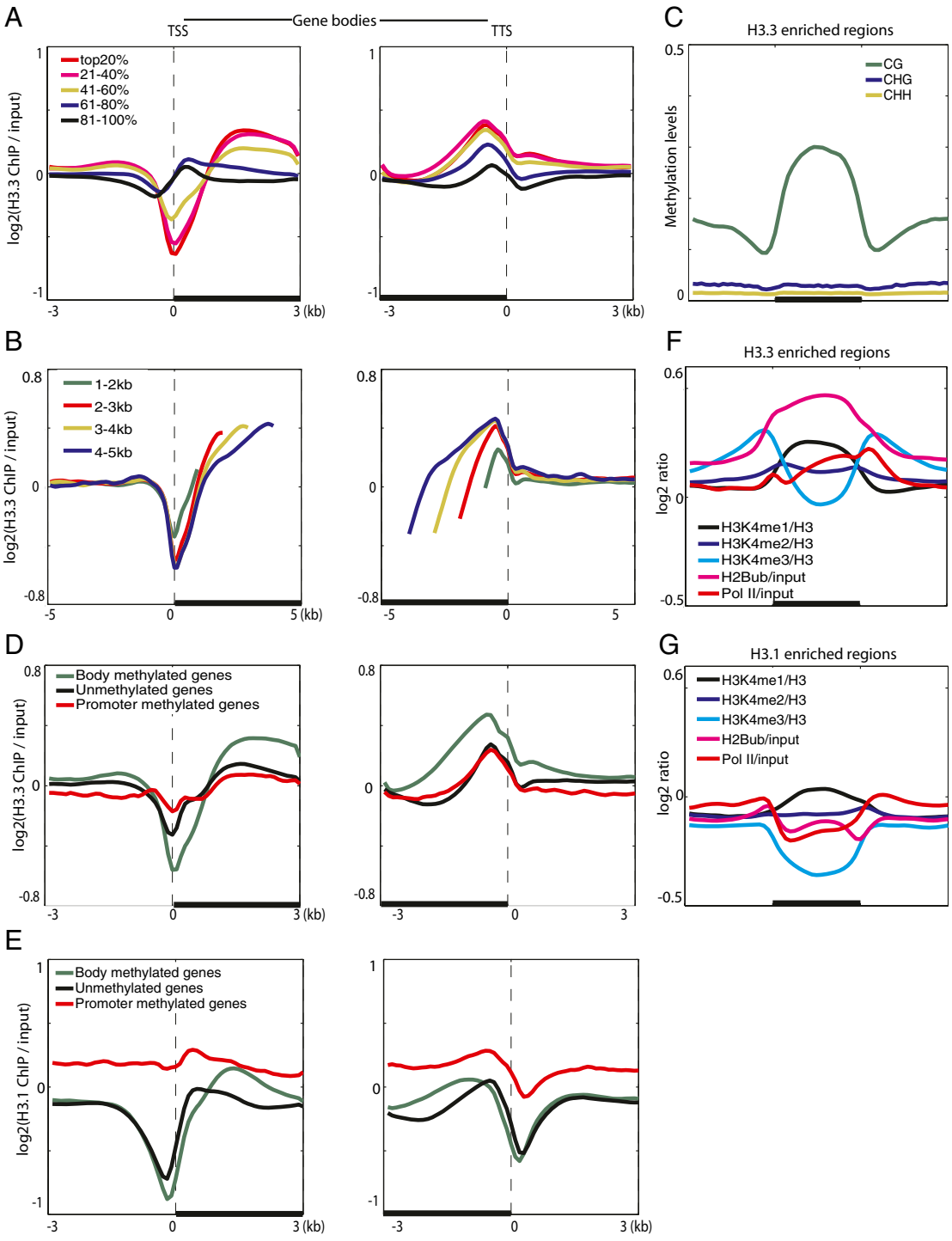

Fig. 3. Genome-wide distribution of H3.3. (*A*) Correlation of H3.3 and gene expression levels. Average distribution of H3.3 reads ± 3 kb relative to transcription start sites (TSS) and transcription termination sites (TTS) are plotted. (*B*) Distribution of H3.3 over genes of different sizes. The *x*-axis is as in *A*. (*C*) Pattern of DNA methylation over H3.3-enriched regions. Flanking regions are the same length as the H3.3 region (middle region). (*D* and *E*) Distribution of H3.3 (*D*) and H3.1 (*E*) over gene body methylated genes, unmethylated genes, and promoter methylated genes. The *x*-axes are as in *A*. (*F* and *G*) Distribution of active chromatin marks over H3.3-enriched (F) and H3.1-enriched (*G*) regions. Flanking regions are the same length as the H3.3 region (middle region).

methylated genes, consistent with its association with transcriptionally silent regions in the genome, and no preference was found in body-methylated genes relative to unmethylated genes (Fig. 3*E*).

Genome-wide analyses in *Drosophila* and humans have suggested some positive correlation between H3.3 and histone H2A.Z, with both enriched near transcription start sites, and there is evidence of the existence of nucleosomes containing both H3.3 and H2A.Z (32, 33). Notably, in *Arabidopsis*, H2A.Z has an antagonistic relationship with DNA methylation and is enriched in 5′ ends of genes (34). To study the relationship between H3.3 and H2A.Z, we defined regions enriched with H2A.Z (34) and examined the distribution of H3.3 over these sites. Consistent with our finding of a positive correlation between DNA methylation and H3.3 (Fig. 3 *C* and *D*), we found that H3.3 is strongly

depleted at sites enriched with H2A.Z, suggesting a negative correlation between H3.3 and H2A.Z in *Arabidopsis* (Fig. S3).

TF-binding sites are enriched at low nucleosome density regions and are depleted over gene bodies (21). Consistent with this finding, we found that both H3.1 and H3.3 are depleted at TF-binding sites (Fig. S4*A*). H3.3 was less depleted than H3.1, possibly related to the association of H3.3 with certain cis-regulatory sites (35). We confirmed depletion of total nucleosome content with Nuc-seq and H3 ChIP-seq datasets, as well as with the nucleosome prediction algorithm (Fig. S4*B*).

We next examined the distributions of active chromatin modifications over H3.3-enriched regions. Consistent with the observation that H3.3 correlates with CG methylation, H3K4me1 (a mark found in the transcribed region of genes) (36) was highly enriched over H3.3 (Fig. 3*F*). Ubiquitinated H2B ChIP (37) and Pol II ChIP (23) signals also were enriched over H3.3, consistent with the presence of H3.3 in active genes (Fig. 3*F*). In contrast, we did not observe these trends with H3.1 (Fig. 3*G*). The positive correlation between H3.3 and Pol II might provide an explanation for the skew of H3.3 toward the 3′ end of genes. H3.3 may be incorporated at sites where chromatin is actively disrupted by elongation of Pol II. Thus, H3.3 is associated with expressed genes, as well as with epigenetic modifications, such as gene body methylation, H3K4me1, and ubiquitinated H2B.

H3 and Origins of Replication. Recently, DNA replication origins in *Arabidopsis* were mapped by sequencing BrdU-labeled DNA from a cultured cell line that can be cell cycle-synchronized (38). Surprisingly, we found that both H3.1 and H3.3 were enriched over these origins (Fig. 4*A*). The enrichment of both types of histones suggests that these origins are generally enriched for nucleosome content. To confirm this, we analyzed nucleosome content by Nuc-seq, H3 ChIP-seq, and the nucleosome prediction algorithm and found strong enrichment for nucleosome content in these origins (Fig. 4*B*). These results suggest that *Arabidopsis* origins are nucleosome-dense. This finding was unexpected, given the association of replication origins with nucleosome-depleted regions (NDRs) in other organisms (39). For instance, in *Drosophila*, the origin recognition complex (ORC) localizes at NDRs (40, 41). In addition, most replication origins in *Saccharomyces cerevisiae* are also associated with NDRs (42), although some efficient origins lack NDRs (43). However, a recent study in *Schizosaccharomyces pombe* found that ORC binding and origins do not overlap with NDR (44). Interestingly, recent proteomic analyses in human cells have suggested that ORC preferentially binds nucleosomes with H3K9m3 or H3K27m3, and that this binding is even more effective in the presence of CpG methylation (45). An attractive hypothesis is that the *Arabidopsis* ORC (38) also binds nucleosomes. An issue to consider is that in the present analysis, origins were defined with cell culture, whereas experimental data from histone enrichment came from seedlings. Proliferating cells in seedlings constitute a small proportion of differentiated cells; thus, a significant proportion of genome sites that work as origins in cultured cells might not be active in seedlings, because cells are no longer proliferating. Thus, until origins in seedlings are mapped, we cannot determine whether nucleosome enrichment is a characteristic of origins that are active or inactive, or both. However, computational predictions of nucleosome occupancy suggest that cell culture replication origins are enriched with nucleosomes, indicating a possible association between nucleosome enrichment and active origins. Our results suggest that nucleosome depletion might not be a conserved characteristic of origins of replication across eukaryotes, and that plant replication origins tend to be nucleosome-enriched.

Conclusions

In the present work, we generated genome-wide maps of two histone H3 variants, H3.1 and H3.3, in *Arabidopsis* and found that H3.1 is associated with transcriptionally silent regions in the genome, whereas H3.3 is associated with transcriptionally active regions and is most highly enriched in the 3′ end of the genes. Notably, we found similar trends as seen in animals, even though H3 variants have evolved independently in plants and animals (7, 8), suggesting convergent evolution.

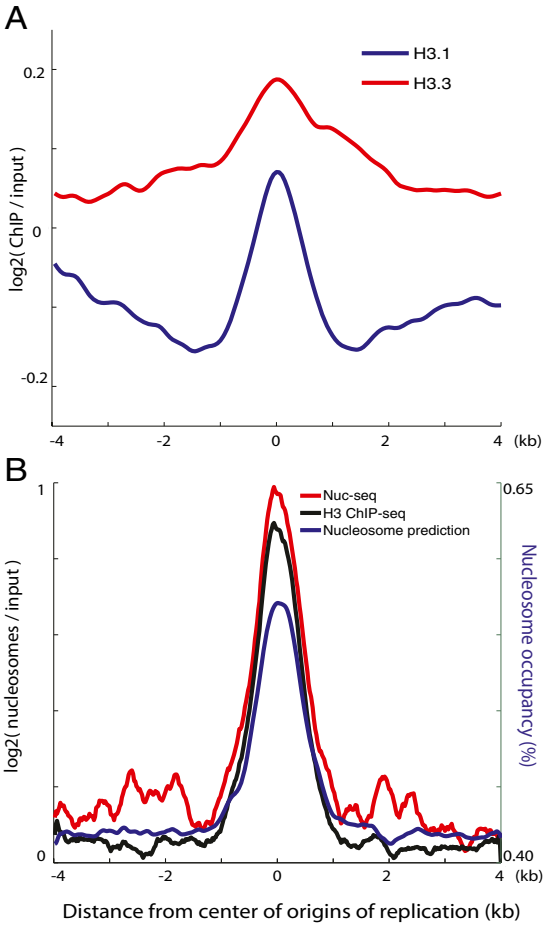

Fig. 4. Enrichment of H3 over origins of replication. (*A*) Distribution of H3.1 and H3.3 over previously defined origins of replication (38). (*B*) Distribution of H3 ChIP-seq, Nuc-seq, and predicted nucleosomes occupancies over origins of replication.

Materials and Methods

Epitope-Tagged *Arabidopsis* Plants. To generate transgenic plants encoding Myc-tagged H3.1 and H3.3 genes, a genomic fragment containing the promoter and the coding region, except for the termination codon, was amplified by PCR using Pfx (Invitrogen) and specific primers containing the *att*B sites (Table S1). PCR products were recombined with pDONR221 (Invitrogen) through a BP recombination reaction to obtain an entry clone, pDONR221-HTR. After a LR recombination reaction (Invitrogen) with destination vector pGWB16 (46), an expression clone with the C-terminal region fused to a Myc tag (4×) was generated (pHTR::HTR:4×Myc). The constructs were introduced into *Agrobacterium tumefaciens* (C58C1 strain), and *Arabidopsis* plants (*A. thaliana* Col-0 ecotype) were transformed by the floral dip method (47). Transformed seeds were selected on Murashige and Skoog agar plates containing kanamycin (50 μg/mL). Plants with only a single insertion were selected, and homozygous plants were used for the analysis. Expression of the Myc-tagged histones was confirmed by Western blot analysis (Fig. S1).

ChIP-seq Library Generation. ChIP-seq assays were performed using 10-d-old seedlings grown in Murashige and Skoog agar plates in a 16-h light/8-h dark regimen at 22 °C. The ChIP experiment was carried out as described previously (48) with minor modifications. Chromatin was sonicated in a Bioruptor (Diagenode) for 30 cycles of 30 s on and 30 s off, and the same amount of chromatin was immunoprecipitated with either 10 μg of anti-Myc antibody (clone 4A6; Millipore) or anti-IgG (ab6703; Abcam) used as a negative control. Illumina

libraries for sequencing were generated, and the libraries were sequenced using the HiSEq 2000 Sequencing System (Illumina), following the manufacturer's instructions.

RNA-seq Library Generation. RNA was extracted from 0.1 g of 10-d-old seedlings using a standard TRIzol method. Total RNA was treated with DNaseI (Roche), and poly(A) purification was performed using the Dynabeads mRNA Purification Kit (Invitrogen). Illumina libraries were generated, and the libraries were sequenced using the HiSEq 2000 Sequencing System (Illumina), following the manufacturer's instructions.

Data Analysis. Sequenced reads were base-called using standard Illumina software. Bowtie (49) was used to uniquely align the reads to the *A. thaliana* genome (*TAIR8*), with up to two mismatches allowed. Reads mapping to identical positions in the genome were collapsed into one read. The numbers of reads obtained for each sample are listed in Table S2. Regions of H3.1 and H3.3 enrichment were defined using the SICER software package (50), with the input genomic DNA as a background control (parameters: W = 200; G = 400; FDR <1E-3). Regions of H3K27me1 ChIP-seq enrichment (19) were defined with SICER, using H3 ChIP-seq reads as a background control (parameters: W = 500; G = 1,500; FDR <0.05). Regions of H2A.Z enrichment (34) were defined by tiling the genome into 500-bp bins (250-bp overlap) and then computing the log2 ratios of the scores of H2A.Z to input genomic DNA. These scores were then *z*-score–transformed, with a cutoff of $z > 2$ cutoff applied. Finally, adjacent H2A.Z-enriched regions were merged. Gene expression levels were determined by calculating reads per kilobase per million mapped reads (51) for each gene. Transcription-binding sites were obtained from AGRIS (http://arabidopsis.med.ohio-state.edu). Plots were normalized for their sequencing depths and smoothed triangularly ($bin_i = 0.25 \times bin_{i-1} + 0.5 \times bin_i + 0.25 \times bin_{i+1}$) fewer than 10 times. Smoothing was performed for presentation purposes and did not affect the conclusions of these experiments.

ACKNOWLEDGMENTS. We thank Fred Berger for discussions and V. Mora-Gil for technical assistance. Research at the C.G. laboratory is supported by Ministry of Science and Education Grants BFU2009-9783 and CSD2007-00057-B and by an institutional grant from Fundación Ramón Areces. S.O. is supported by a Junta de Ampliacion de Estudios Predoctoral Fellowship from the Consejo Superior de Investigaciones Cientificas. The research at the S.E.J. laboratory was supported by National Science Foundation Grant MCB-1121245. H.S. was supported by a Fred Eiserling and Judith Lengyel Graduate Doctoral Fellowship. S.E.J. is an Investigator of the Howard Hughes Medical Institute.

1. Elsaesser SJ, Goldberg AD, Allis CD (2010) New functions for an old variant: No substitute for histone H3.3. *Curr Opin Genet Dev* 20:110–117.
2. Deal RB, Henikoff S (2011) Histone variants and modifications in plant gene regulation. *Curr Opin Plant Biol* 14:116–122.
3. Loyola A, Almouzni G (2007) Marking histone H3 variants: How, when and why? *Trends Biochem Sci* 32:425–433.
4. Talbert PB, Henikoff S (2010) Histone variants—ancient wrap artists of the epigenome. *Nat Rev Mol Cell Biol* 11:264–275.
5. Goldberg AD, et al. (2010) Distinct factors control histone variant H3.3 localization at specific genomic regions. *Cell* 140:678–691.
6. Ahmad K, Henikoff S (2002) The histone variant H3.3 marks active chromatin by replication-independent nucleosome assembly. *Mol Cell* 9:1191–1200.
7. Ingouff M, Berger F (2010) Histone 3 variants in plants. *Chromosoma* 119:27–33.
8. Waterborg JH (2011) Evolution of histone H3: Emergence of variants and conservation of post-translational modification sites. *Biochem Cell Biol* 90(1):79–95.
9. Shi L, Wang J, Hong F, Spector DL, Fang Y (2011) Four amino acids guide the assembly or disassembly of *Arabidopsis* histone H3.3-containing nucleosomes. *Proc Natl Acad Sci USA* 108:10574–10578.
10. Wirbelauer C, Bell O, Schübeler D (2005) Variant histone H3.3 is deposited at sites of nucleosomal displacement throughout transcribed genes while active histone modifications show a promoter-proximal bias. *Genes Dev* 19:1761–1766.
11. Mito Y, Henikoff JG, Henikoff S (2005) Genome-scale profiling of histone H3.3 replacement patterns. *Nat Genet* 37:1090–1097.
12. Mishiba K, et al. (2005) Consistent transcriptional silencing of 35S-driven transgenes in gentian. *Plant J* 44:541–556.
13. Thomas CE, Kelleher NL, Mizzen CA (2006) Mass spectrometric characterization of human histone H3: A bird's eye view. *J Proteome Res* 5:240–247.
14. Johnson L, et al. (2004) Mass spectrometry analysis of *Arabidopsis* histone H3 reveals distinct combinations of post-translational modifications. *Nucleic Acids Res* 32:6511–6518.
15. Okada T, Endo M, Singh MB, Bhalla PL (2005) Analysis of the histone H3 gene family in *Arabidopsis* and identification of the male-gamete–specific variant AtMGH3. *Plant J* 44:557–568.
16. Ingouff M, et al. (2010) Zygotic resetting of the HISTONE 3 variant repertoire participates in epigenetic reprogramming in *Arabidopsis*. *Curr Biol* 20:2137–2143.
17. Jacob Y, et al. (2009) ATXR5 and ATXR6 are H3K27 monomethyltransferases required for chromatin structure and gene silencing. *Nat Struct Mol Biol* 16:763–768.
18. Bernatavichute YV, Zhang X, Cokus S, Pellegrini M, Jacobsen SE (2008) Genome-wide association of histone H3 lysine nine methylation with CHG DNA methylation in *Arabidopsis thaliana*. *PLoS ONE* 3:e3156.
19. Jacob Y, et al. (2010) Regulation of heterochromatic DNA replication by histone H3 lysine 27 methyltransferases. *Nature* 466:987–991.
20. Feng S, Jacobsen SE (2011) Epigenetic modifications in plants: An evolutionary perspective. *Curr Opin Plant Biol* 14:179–186.
21. Zhang X, et al. (2007) Whole-genome analysis of histone H3 lysine 27 trimethylation in *Arabidopsis*. *PLoS Biol* 5:e129.
22. Turck F, et al. (2007) *Arabidopsis* TFL2/LHP1 specifically associates with genes marked by trimethylation of histone H3 lysine 27. *PLoS Genet* 3:e86.
23. Chodavarapu RK, et al. (2010) Relationship between nucleosome positioning and DNA methylation. *Nature* 466:388–392.
24. Kaplan N, et al. (2009) The DNA-encoded nucleosome organization of a eukaryotic genome. *Nature* 458:362–366.
25. Ooi SL, Henikoff JG, Henikoff S (2010) A native chromatin purification system for epigenomic profiling in *Caenorhabditis elegans*. *Nucleic Acids Res* 38:e26.
26. Tran RK, et al. (2005) DNA methylation profiling identifies CG methylation clusters in *Arabidopsis* genes. *Curr Biol* 15:154–159.
27. Zhang X, et al. (2006) Genome-wide high-resolution mapping and functional analysis of DNA methylation in *Arabidopsis*. *Cell* 126:1189–1201.
28. Zilberman D, Gehring M, Tran RK, Ballinger T, Henikoff S (2007) Genome-wide analysis of *Arabidopsis thaliana* DNA methylation uncovers an interdependence between methylation and transcription. *Nat Genet* 39:61–69.
29. Cokus SJ, et al. (2008) Shotgun bisulphite sequencing of the *Arabidopsis* genome reveals DNA methylation patterning. *Nature* 452:215–219.
30. Feng S, et al. (2010) Conservation and divergence of methylation patterning in plants and animals. *Proc Natl Acad Sci USA* 107:8689–8694.
31. Zemach A, McDaniel IE, Silva P, Zilberman D (2010) Genome-wide evolutionary analysis of eukaryotic DNA methylation. *Science* 328:916–919.
32. Henikoff S, Henikoff JG, Sakai A, Loeb GB, Ahmad K (2009) Genome-wide profiling of salt fractions maps physical properties of chromatin. *Genome Res* 19:460–469.
33. Jin C, et al. (2009) H3.3/H2A.Z double-variant–containing nucleosomes mark "nucleosome-free regions" of active promoters and other regulatory regions. *Nat Genet* 41:941–945.
34. Zilberman D, Coleman-Derr D, Ballinger T, Henikoff S (2008) Histone H2A.Z and DNA methylation are mutually antagonistic chromatin marks. *Nature* 456:125–129.
35. Mito Y, Henikoff JG, Henikoff S (2007) Histone replacement marks the boundaries of cis-regulatory domains. *Science* 315:1408–1411.
36. Zhang X, Bernatavichute YV, Cokus S, Pellegrini M, Jacobsen SE (2009) Genome-wide analysis of mono-, di- and trimethylation of histone H3 lysine 4 in *Arabidopsis thaliana*. *Genome Biol* 10:R62.
37. Roudier F, et al. (2011) Integrative epigenomic mapping defines four main chromatin states in *Arabidopsis*. *EMBO J* 30:1928–1938.
38. Costas C, et al. (2011) Genome-wide mapping of *Arabidopsis thaliana* origins of DNA replication and their associated epigenetic marks. *Nat Struct Mol Biol* 18:395–400.
39. Meisch F, Prioleau MN (2011) Genomic approaches to the initiation of DNA replication and chromatin structure reveal a complex relationship. *Brief Funct Genomics* 10:30–36.
40. MacAlpine HK, Gordân R, Powell SK, Hartemink AJ, MacAlpine DM (2010) *Drosophila* ORC localizes to open chromatin and marks sites of cohesin complex loading. *Genome Res* 20:201–211.
41. Deal RB, Henikoff JG, Henikoff S (2010) Genome-wide kinetics of nucleosome turnover determined by metabolic labeling of histones. *Science* 328:1161–1164.
42. Eaton ML, Galani K, Kang S, Bell SP, MacAlpine DM (2010) Conserved nucleosome positioning defines replication origins. *Genes Dev* 24:748–753.
43. Halpin C (2005) Gene stacking in transgenic plants—the challenge for 21st century plant biotechnology. *Plant Biotechnol J* 3:141–155.
44. de Castro E, et al. (2012) Nucleosomal organization of replication origins and meiotic recombination hotspots in fission yeast. *EMBO J* 31:124–137.
45. Bartke T, et al. (2010) Nucleosome-interacting proteins regulated by DNA and histone methylation. *Cell* 143:470–484.
46. Nakagawa T, et al. (2007) Development of series of gateway binary vectors, pGWBs, for realizing efficient construction of fusion genes for plant transformation. *J Biosci Bioeng* 104:34–41.
47. Clough SJ, Bent AF (1998) Floral dip: A simplified method for *Agrobacterium*-mediated transformation of *Arabidopsis thaliana*. *Plant J* 16:735–743.
48. Villar CB, Köhler C (2010) Plant chromatin immunoprecipitation. *Methods Mol Biol* 655:401–411.
49. Langmead B (2010) Aligning short sequencing reads with Bowtie. *Curr Protoc Bioinform* 32:11.7.1–11.7.14.
50. Zang C, et al. (2009) A clustering approach for identification of enriched domains from histone modification ChIP-Seq data. *Bioinformatics* 25:1952–1958.
51. Mortazavi A, Williams BA, McCue K, Schaeffer L, Wold B (2008) Mapping and quantifying mammalian transcriptomes by RNA-Seq. *Nat Methods* 5:621–628.